AGU PUBLICATIONS

JGR

Journal of Geophysical Research: Atmospheres

RESEARCH ARTICLE

10.1002/2017JD027543

Key Points:
- Nepal can be divided into three regions of similar daily precipitation characteristics
- We identify synoptic conditions related to extreme precipitation in Nepal and pinpoint regions of additional moisture sources contributing to extreme events
- A conceptual sketch of the involved processes concludes our findings

Correspondence to:
P. Bohlinger,
patrik.bohlinger@uib.no

Citation:
Bohlinger, P., Sorteberg, A., & Sodemann, H. (2017). Synoptic conditions and moisture sources actuating extreme precipitation in Nepal. *Journal of Geophysical Research: Atmospheres*, *122*, 12,653–12,671. https://doi.org/10.1002/2017JD027543

Received 1 AUG 2017
Accepted 8 NOV 2017
Accepted article online 14 NOV 2017
Published online 7 DEC 2017

Synoptic Conditions and Moisture Sources Actuating Extreme Precipitation in Nepal

Patrik Bohlinger[1,2], Asgeir Sorteberg[1,2], and Harald Sodemann[1,2]

[1]Geophysical Institute, University of Bergen, Bergen, Norway, [2]Bjerknes Centre for Climate Research, University of Bergen, Bergen, Norway

Abstract Despite the vast literature on heavy-precipitation events in South Asia, synoptic conditions and moisture sources related to extreme precipitation in Nepal have not been addressed systematically. We investigate two types of synoptic conditions—low-pressure systems and midlevel troughs—and moisture sources related to extreme precipitation events. To account for the high spatial variability in rainfall, we cluster station-based daily precipitation measurements resulting in three well-separated geographic regions: west, central, and east Nepal. For each region, composite analysis of extreme events shows that atmospheric circulation is directed against the Himalayas during an extreme event. The direction of the flow is regulated by midtropospheric troughs and low-pressure systems traveling toward the respective region. Extreme precipitation events feature anomalous high abundance of total column moisture. Quantitative Lagrangian moisture source diagnostic reveals that the largest direct contribution stems from land (approximately 75%), where, in particular, over the Indo-Gangetic Plain moisture uptake was increased. Precipitation events occurring in this region before the extreme event likely provided additional moisture.

1. Introduction

Recent studies found considerable changes in extreme precipitation in Nepal over the last 40 years (Baidya et al., 2008; Caesar et al., 2011; Shrestha et al., 2016). Bohlinger and Sorteberg (2017) pointed to a statistically robust trend of increasing rainfall extremes in west Nepal, stressing the need to better understand the involved processes. However, despite vast literature on heavy-precipitation events in South Asia, the role of synoptic conditions and moisture sources for extreme precipitation events in Nepal has not been addressed systematically. As described by Trenberth et al. (2003), three overarching constituents are crucial for generating precipitation: ascending air tied to dynamics on different scales (from planetary scale to synoptic scale and mesoscale), microphysics that determine the condensation process, and the presence of moisture. We assess the role of synoptic conditions and moisture sources and how they effect extreme precipitation in Nepal.

The spatial precipitation distribution in Nepal exhibits high spatial and temporal variability and is therefore of high socioeconomic interest due to agriculture, natural hazards, and the use of hydropower. Precipitation in Nepal is heavily influenced by the Indian summer monsoon (Bohlinger & Sorteberg, 2017). Based on meteorological stations, early studies estimated the average monsoon precipitation to be approximately 80% of the annual precipitation across most of Nepal (Nayava, 1980). In the far western part, the proportion reached only about 60%. Nepal exhibits a spatial pattern of rainfall climatologies according to its physiographic regions and main river systems (Kansakar et al., 2004). A correlation between elevation and precipitation was found in west Nepal, whereas the middle and east show no clear dependency (Ichiyanagi et al., 2007). However, the rainfall distribution in Nepal is more complex and exhibits large differences on small scales; for example, a difference by a factor of 8 in precipitation amounts was observed in the Marsyandi river basin in Nepal (factor of 4 on a scale of 10 km) (Barros & Lang, 2003; Lang & Barros, 2002). A systematic approach should therefore take into account the spatial variability of precipitation when attributing synoptic conditions to extreme precipitation events.

Typical synoptic conditions leading to heavy precipitation in Nepal have been summarized to the following: monsoon low-pressure systems, break monsoon conditions, western disturbances, and a change in the seasonal monsoon trough (Nandargi & Dhar, 2011). This summary is largely based on studies of single events with impact along the Himalayas. The listed features can act on different regions along the Himalayas

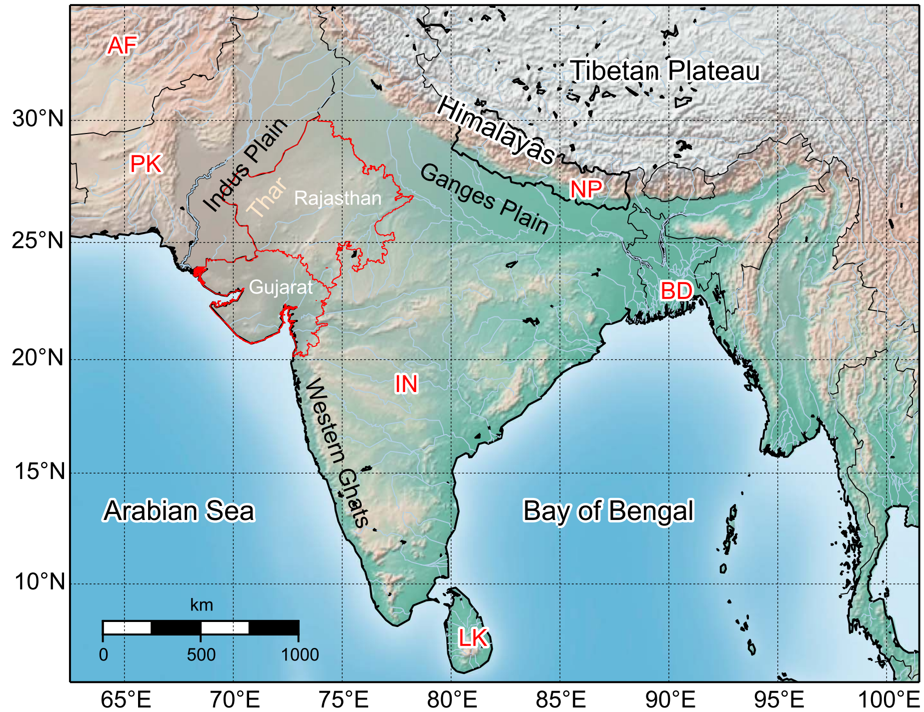

Figure 1. Overview map for South Asia including India (IN), Pakistan (PK), Afghanistan (AF), Bangladesh (BD), and Sri Lanka (LK). Nepal (NP) is located at the rim of the Himalayas and marked with thicker borders. The Indian states Rajasthan and Gujarat are indicated in red for further discussion. Main rivers are colored blue and follow the main basins, Indus Plain and Ganges Plain (together called Indo-Gangetic Plain). The location of the Thar Desert is indicated with light brown font; the Western Ghats are indicated in black font.

and are dominant in different months. For instance, in central Nepal, mesoscale systems are found to strongly interact with steep terrain at elevations of 1 – 2 km (Barros et al., 2000) where during the monsoon onset, monsoon depressions from the Bay of Bengal (Figure 1) can move close to the Himalayan mountain range and force air upslope causing precipitation (Lang & Barros, 2002). However, implications of these studies for Nepal and where to expect which of the synoptic conditions are not clear.

Another approach in the literature was to relate the occurrence of different convective systems to synoptic anomalies for various regions along the Himalayas (Romatschke & Houze, 2011). Nepal was part of a larger region called central Himalayan foothills and therefore not discussed in detail. For the central Himalayan foothills, trough conditions over the Tibetian Plateau and positive anomalies south of the Himalayas favored medium convective systems. Houze et al. (2007) described various mechanisms triggering monsoon convection in the Himalayas, emphasizing a strong interaction with the complex terrain and regional differences between west, central, and east Himalayas. Over the west Himalayas a key feature was a cap of dry air flowing down from the Afghan Plateau (Figure 1). This cap prevented premature triggering of convection of moist air coming from the Arabian Sea (first described by Sawyer, 1947). As the moist air masses approach the Himalayas they are orographically lifted, finally triggering convection. This was later confirmed by Medina et al. (2010) in numerical model experiments. Such a systematic assessment remains to be conducted for synoptic conditions related to extreme precipitation along the Nepalese Himalayas.

The second constituent for precipitation addressed in our study is the availability of precipitable water. This directly connects to the location and contribution of moisture sources raising the following question: if there is more moisture precipitating, where does the additional moisture come from? However, various studies investigated the origin of moisture for the Indian subcontinent. Ghosh et al. (1978) derived water vapor flux from airborne measurements along different transects in the Arabian Sea concluding that evaporation along the Arabian Sea is a major moisture source. Cadet and Reverdin (1981) investigated surface water vapor transport for the 1975 summer monsoon season using a budget approach based on cross sections. They state that during the monsoon season as much as 70% of the water vapor crossing the west coast of India could originate in the Southern Hemisphere, while the remaining 30% evaporate from the Arabian Sea. Moisture picked up

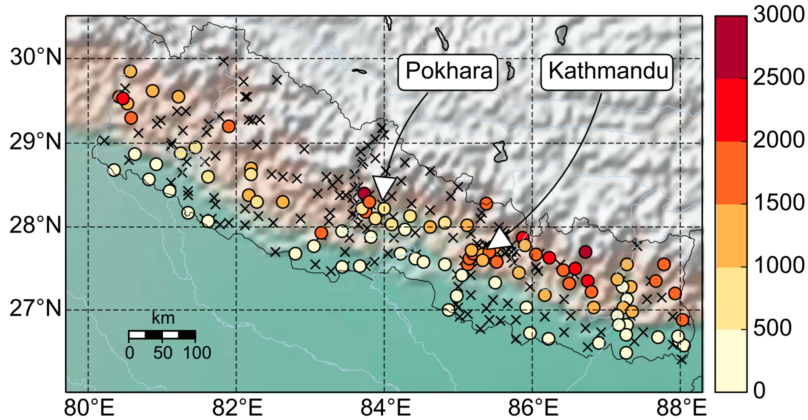

Figure 2. The location of 278 meteorological stations from the Department of Hydrology and Meteorology (DHM) in Nepal. Stations we use for our analysis are displayed with circles, and their elevation is given in meters above sea level (m asl). Disregarded stations in our study are marked with a cross. Regions with comparable high density population, Pokhara and the capital Kathmandu, have also a higher station density. Rivers are colored blue.

by traversing air masses over the Indian Ocean in the Bay of Bengal would mainly contribute to the development of local weather phenomena. Later studies confirmed these findings and stress the importance of the Arabian Sea and the Southern Hemisphere as moisture sources (Cadet & Greco, 1987; Wang, 2005). However, implications for moisture sources for Nepal are not clear and need to be addressed separately. To our knowledge there is no study assessing moisture sources for extreme precipitation in Nepal.

Research on single high-impact events close to the Nepalese Himalayas hints to synoptic processes and moisture sources possibly applicable for Nepal. In particular, the city of Leh flood 2010 (Kumar et al., 2014; Rasmussen & Houze, 2012) and floods in Pakistan (Houze et al., 2011; Martius et al., 2013; Medina et al., 2010; Rasmussen et al., 2015) were explored. For the city of Leh flood 2010, moisture from the Arabian Sea and the Bay of Bengal was funneled to Leh and fed into mesoscale convective systems moving down from the Himalayan Plateau (Rasmussen & Houze, 2012). For the Pakistan flood in 2010, Martius et al. (2013) found that orographical lifting and atmospheric flow directed against the Himalayan mountain chain was a main driver. Using the moisture source diagnostic from Sodemann et al. (2008), they found a considerable contribution from land, over India and Pakistan, and from the Arabian sea. The scope of their study did not include the mechanism by which a large amount of moisture could be taken up over an otherwise relatively dry land area like the Thar Desert (Figure 1). However, they proposed a possible intense coupling of precipitation and evapotranspiration. It is not known whether similar mechanisms prevail during extreme precipitation in Nepal. Therefore, we address systematically regional aspects and explore the moisture sources in conjunction with the synoptic conditions leading to extreme precipitation over Nepal.

2. Data

We used data from meteorological stations provided by the Department of Hydrology and Meteorology (DHM) in Nepal measuring 24 h precipitation sums (from 9 a.m. to 9 a.m. local time). We picked 112 stations (Figure 2) that remain after data availability control with constraints from Bohlinger and Sorteberg (2017). The main criterion for choosing a station was that every month in the monsoon season June to September should have 75% of valid data for at least 30 years in the period 1971 to 2010. The 112 chosen stations are well distributed over the country and cover most of the climatic zones as defined in Shrestha et al. (2016). The capital, Kathmandu, and the city Pokhara stand out from the otherwise sparsely covered country as more stations are located close by (Figure 2).

We used two additional data sets for our analysis: 6-hourly Era-Interim reanalysis (Dee et al., 2011) at 0.75° horizontal resolution and a global particle trajectory data set consisting of 5 million particles of equal mass representing the entire atmosphere (from 1979 to 2013) (Läderach & Sodemann, 2016). This data set was computed with the Lagrangian dispersion model FLEXPART (Stohl et al., 2005) based on Era-Interim reanalysis fields.

3. Methods

3.1. Clustering of the Rain Gauge Stations

We cluster our station-based precipitation records to find groups of stations that behave similarly in terms of precipitation changes. As distance metric for the *K*-means algorithm with random seeding, we use correlation between the rain gauge stations based on daily precipitation amounts during 30 years of monsoon seasons. This distance metric is chosen since daily precipitation is not Gaussian distributed. A typical dilemma with cluster algorithms is that one has to know the number of clusters beforehand. There are different approaches to face this problem, but the alleged objective methods still need subjective judgment. The methods we used to decide whether a chosen number of cluster was suitable were comparison of silhouettes (Rousseeuw, 1987), aiming for high silhouette coefficients, and applying gap statistics (Tibshirani et al., 2001).

3.2. Identification of Low-Pressure Systems

We identified and tracked low-pressure systems (LPS) using the Lagrangian tracking algorithm (Hodges, 1994, 1995, 1999). This algorithm is fed with relative vorticity from ERA-Interim (Dee et al., 2011) on the Gaussian grid F128 and follows the relative vorticity maximum on 850 hPa. At this pressure level monsoon LPS are expected to exhibit a vorticity maximum (Tyagi et al., 2012). We further consider only systems that last longer than 2 days, travel more than 1000 km, and exceed a vorticity threshold of $5 \cdot 10^{-6}\ s^{-1}$. This tracking algorithm has already been successfully applied for monsoon LPS in South Asia (Sørland & Sorteberg, 2015a).

3.3. Identification of Moisture Source Regions

We assess moisture changes along each trajectory from Läderach and Sodemann (2016) with the moisture source diagnostic from Sodemann et al. (2008). This diagnostic method allows the attribution of moisture sources by relating each moisture gain or loss along an air parcel trajectory to the current-specific humidity of the same air parcel. In this methodology, moisture loss counts as precipitation. We follow the trajectory 10 days prior to the extreme event, which explains on average 91% of the moisture changes over Nepal. This means that on average 9% of the moisture in the air parcel was already present when starting the diagnostic and therefore cannot be attributed. The high fraction of explained moisture changes gives confidence in the applicability of the method in this area with limitations discussed in the next paragraph. We compute moisture sources only for trajectories that lose moisture (>0.1 mm) in the target region and by this only quantify sources relevant for precipitation.

The attribution of moisture uptake is divided into two vertical layers (Sodemann et al., 2008): contribution from the boundary layer and the free troposphere. Boundary layer contribution consists of all uptake below 1.5 times the boundary layer height in Era-Interim. Consequently, everything above is defined as uptake in the free troposphere. This division is due to the assumption that within the boundary layer vertical mixing is much stronger than horizontal advection. The origin of the taken up moisture corresponds to the location of the parcel which is here defined as the moisture source region. This assumption is less obvious in the free troposphere where moisture can be advected from far away or introduced by plumes of convection and evaporating rain. For the moisture diagnostic we use 6-hourly steps for recalculating the budget for the respective air parcel. During this 6 h the parcel could cross a convective plume which would change its moisture content. In this study we only take into account the contribution from the planetary boundary layer to assess the contribution of regions over which moisture was picked up by an air parcel.

Winschall et al. (2014) compared the Lagrangian moisture source diagnostic against a Eulerian moisture source diagnostic using the limited area model COSMO with water vapor tracers. They focused on a heavy-precipitation event leading to the flood in eastern Europe in May 2010 and found that both approaches are generally consistent. They concluded that the Lagrangian moisture source diagnostic from Sodemann et al. (2008) is a computationally efficient tool for determining moisture source regions. Läderach (2016) investigated the moisture transport to Kathmandu for a case study (22 days). He compared the Lagrangian diagnostic with Eulerian model results and concluded with a good agreement in this region, strengthening confidence in our approach.

To attribute moisture sources to extreme precipitation events we divided Nepal into west, central, and east Nepal (Figure 2). The area of Nepal was determined by the area within 26–31°N and 79–89°E. West Nepal was defined as 27.5–30.5°N and 80–83.5°E, Central Nepal as 26.5–29°N and 83–86°E, and East Nepal as 26–28.5°N and 85.5–88.5°E. For the discussion on moisture in the Thar Desert, we chose an area in the Indian state Rajasthan defined as 25–28°N and 71–75°E. For all target regions we tracked air parcels back in time

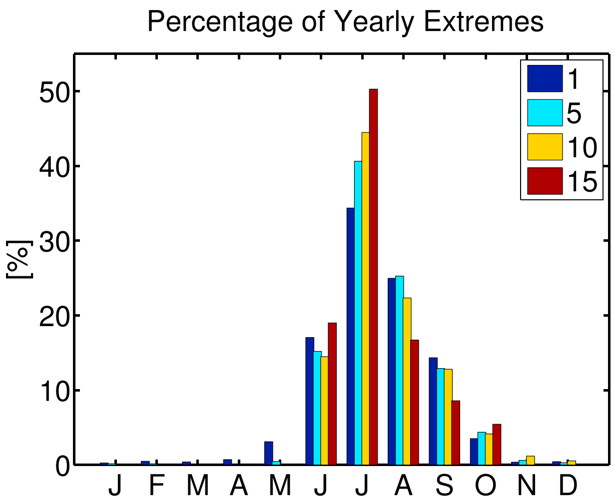

Figure 3. Monthly contribution to annual number of extreme events (in percent) for a minimum of 1, 5, 10, or 15 stations indicating extreme precipitation at the same day.

for 10 days to quantify their moisture sources. Only air parcels that enter through the above defined borders and lose moisture in the target region are tracked.

3.4. Definition of Anomalies and Extremes

The Indian summer monsoon is a transient feature with high variability in the onset date, the progression, and strength. Therefore, the mean state of the Indian summer monsoon is not representative as a reference field. Hence, anomalies are calculated as the difference between an event and a mean background state consisting of a 15 day average centered around the date of the event.

We focus on synoptic conditions related to precipitation events exceeding the threshold of the 99.5th percentile. We call these events for the rest of the study extreme events as they are far out in the tale of the distribution of daily precipitation. Figure 3 illustrates that Nepal experiences most extremes simultaneously at multiple stations during the Indian summer monsoon. Bohlinger and Sorteberg (2017) found that the monsoon is the dominating season for the exceedance of high percentiles. They further point out that a relationship between the number of extreme events and the El Niño–Southern Oscillation (ENSO) have no significant linear correlation above the 99th percentile. Thus, we do not need to treat extreme events in ENSO years in a special way. Exemplary time series of extreme events and the correlation with ENSO together with trends and climatology can be viewed in Bohlinger and Sorteberg (2017). Choosing at least five stations indicating an extreme event should serve as division between very localized convective events and larger-scale systems that trigger extreme precipitation at several stations simultaneously.

We pick a date whenever extreme precipitation is observed at a minimum of five stations on the same day (329 dates). Based on this constraint, we select extreme dates for each cluster (section 4). We further exclude all extremes that occurred simultaneously at more than one cluster which leaves us 231 dates to obtain region-specific characteristics. This means that roughly 70% of all extreme dates were confined to a single cluster. Additionally, we remove all dates prior to the start of Era-Interim in 1979 and use only dates between June and September. This results in 180 dates (cluster 1, 51; cluster 2, 77; and cluster 3, 52) which, despite the thinning process, contain high-impact events like 19/20 July 1993 and 30 August 1998 (Chalise & Khanal, 2002) in the second cluster. From the set of remaining dates we create composites of geopotential height to capture features of atmospheric dynamics (section 6).

A limitation of this approach is that due to the seasonal climate of Nepal, most of the extreme events fall within the monsoon season where also most of the annual precipitation falls (Bohlinger & Sorteberg, 2017). This leads to an overrepresentation of dates with extreme events during the monsoon season. However, these are extreme events with considerable amounts of precipitation meaning that they are likely to be of greater importance to society. This and the fact that contemporaneous extreme events at multiple stations are concentrated in the monsoon seasons (Figure 3) are reasons for us to focus on the monsoon season. Extremes relative to different seasons could be discussed separately in another study.

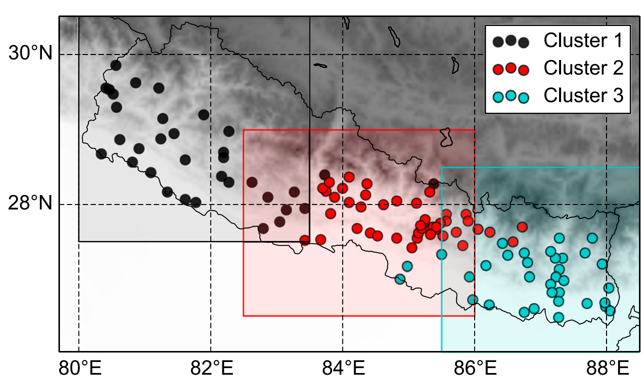

Figure 4. Result of *K*-means clustering with the distance metric correlation on precipitation raw data. Regions for the clusters used for moisture sources are filled in the respective colors. Topography is shaded in gray for orientation.

4. Regimes of Daily Precipitation in Nepal

Due to the large variety of processes leading to heavy-precipitation events (Nandargi & Dhar, 2011) and the spatial variability discussed in section 1, we divide Nepal into subregions using clustering. By this, we can focus on the processes for each subregion with less probability of averaging out important features. Gap statistics suggest a best gain of information for two or three clusters. Due to the distribution of the silhouettes for two and three clusters, we decide for the latter which leads to a division of Nepal into three well-defined regions (Figure 4).

The obtained clusters display a division into west, central, and east Nepal. This division is similar to results obtained by Kansakar et al. (2004) where precipitation regimes followed major drainage basins Karnali, Narayani, and Sapta Koshi. This is striking because their approach differs from ours in various significant points. They applied a hierarchical, agglomerative cluster analysis to classify precipitation regimes in Nepal on a climate time scale. They clustered separately "shape" and "magnitude" as originally proposed by Hannah et al. (2000). The classification using the stations' magnitude was based on climatic time scale variables such as mean, minimum, and maximum, whereas clustering shape was based on monthly z scores to produce an annual precipitation with values of similar magnitude for each station. Kansakar et al. (2004) first divided Nepal into physiographic regions and major drainage basins resulting in six regions and subsequently found the dominating precipitation type for this region. This differs substantially from our approach where we focus on classifying stations using daily precipitation amounts in order to cluster stations that react concurrently to a synoptic scale forcing. We further did not impose any constraints on the clustering and yet our study results in a similar division.

This robust result emerging from clustering station precipitation could be related to larger-scale systems triggering precipitation in the respective region. When increasing the number of clusters, the stations divide into regions parallel to the Himalayas while mostly retaining the perpendicular division (not shown). Various studies (Barros et al., 2000; Barros & Lang, 2003; Bookhagen & Burbank, 2006, 2010; Houze et al., 2007; Lang & Barros, 2002) illustrate a strong influence of topography on precipitation. The observed division of the clusters parallel to the mountain chain could mirror the influence of topography and how far weather systems are able to penetrate into the mountain chain. A more detailed discussion on the sensitivity of the results due to changes in the method or ingoing data can be read in Appendix A. We investigate in the coming sections whether the synoptic conditions differ between extreme precipitation events occurring in the cluster regions.

5. Atmospheric Circulation and Moisture Sources for Nepal During the Monsoon

During the Indian summer monsoon, typically a surface low-pressure area prevails over the Indo-Gangetic Plain covering north India and the northern Bay of Bengal (e.g., Tyagi et al., 2012; Wang, 2005). This is known as the monsoon trough. A band of high geopotential height with anticyclonic flow dominates the upper troposphere at 200 hPa (e.g., Houze et al., 2007; Romatschke et al., 2010) reaching from the Arabian Peninsula to Bangladesh along the Himalayas. This zone of low-level convergence and upper level divergence represents the northward shifted Intertropical Convergence Zone (ITCZ) during the Indian summer monsoon. In the midtroposphere, a center of low geopotential height resides over northeast India and the Bay of Bengal (Figure 5a). Winds follow the geopotential height and veer toward north over the Bay of Bengal. Over Nepal, the low-level atmospheric flow changes direction from northwesterly to southeasterly and is consequently steered against the Himalayas (Figure 5b). In the lower troposphere, an area of low geopotential height (Figure 5b) extends from Pakistan to Bangladesh following the Indo-Gangetic Plain. This region of low geopotential height coincides with the location of LPS that form during the monsoon season and can influence the strength and direction of the moisture transport (Krishnamurthy & Ajayamohan, 2010; Sørland & Sorteberg, 2015b).

Averaged over the entire monsoon season, the vertically integrated moisture transport is aligned with the surface winds and depicts a strong band from the region of the Somali jet, crossing the Western Ghats in India (Figure 1), and turning north in the Bay of Bengal (Figure 6a). During the Indian summer monsoon the area with the strongest vertical integrated moisture transport is located over the Indian Ocean in the Southern Hemisphere close to the equator, over the Arabian Sea, over Sri Lanka, and in the Bay of Bengal. Moisture is steered toward the Himalayan mountain chain where the flow follows the topography and bifurcates, one branch to the northwest along the Nepal Himalayas and one to the northeast (Figure 6a). Viewing the integrated moisture transport during the monsoon season in Figure 6a creates the notion that most of the moisture that precipitates along the Himalayas during the monsoon stems from the Bay of Bengal, the Arabian Sea, or as far as south of the equator. Focusing on moisture sources for the Indian subcontinent, this has in fact been shown in multiple studies which describe the magnitude of the moisture uptake over the ocean (Cadet & Greco, 1987; Cadet & Reverdin, 1981; Ghosh et al., 1978; Wang, 2005, Chapters 1 and 4). Their findings are based on a moisture budget approach investigating vertically integrated moisture fluxes or comparing evaporation with precipitation deducted from measurements. They find that during the monsoon

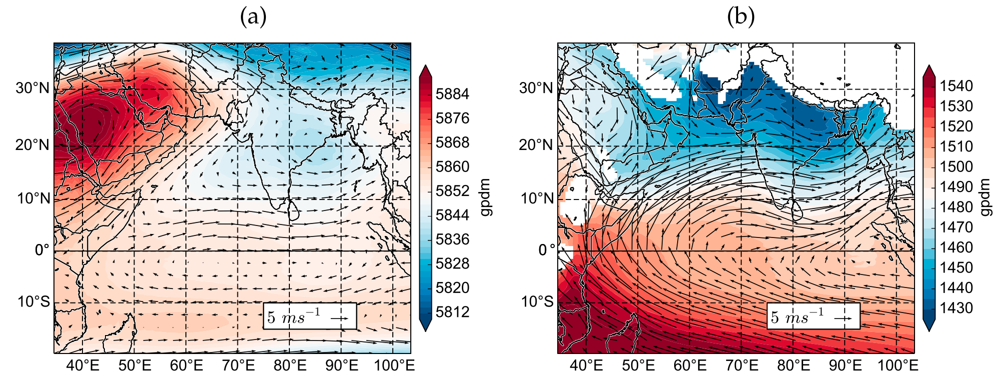

Figure 5. Geopotential height from Era-Interim averaged for June to September from 1979 to 2010 at (a) 500 hPa and (b) 850 hPa. The geopotential height contours are in geopotential decameters (gpdm), and arrows depict the wind at the respective levels.

season water vapor crossing the west coast of India stems mainly from the Southern Hemisphere (70%) and the Arabian Sea (30%).

With Figure 6a in mind, one could conclude that the moisture sources are similar for Nepal. Our results challenge this notion when exploring moisture sources computed using the Lagrangian moisture source diagnostic (Figure 6b). The method reveals that most of the moisture precipitating over Nepal is taken up along the Indo-Gangetic Plain north of the main branch of moisture transport in Era-Interim. We find that around 25% of all relevant uptake (solid black line) occurs over Nepal and the direct vicinity. Roughly 50% (stippled black line) stem from the Indo-Gangetic Plain. In total, 80% of the moisture is taken up over land and 20% over the ocean. Long-range transport seems to be relevant for a large fraction of the 20% as it originates mainly from the Arabian Sea (15%) and off the coast of Somalia (details in Table 1).

We suggest that the reason for the difference between results from the budget approach and our results, obtained with the Lagrangian method, is that the budget approach cannot take into account recycling of moisture. The budget approach compares all evaporated moisture with all precipitation within certain borders or a volume. This can describe whether a region on average acts as a moisture source but cannot attribute moisture sources contributing to a certain precipitation event. Specifically for Nepal, this could mean that originally the moisture had been taken up over sea but thereafter, due to multiple rain events on the way to Nepal, the moisture that stemmed from the Arabian Sea had left the air parcel and was gradually replaced by moisture taken up over land. Hence, the direct source for the specific precipitation event over Nepal was over land. This chain of events would be masked in a budget approach. It becomes clear that the results of the two different approaches are not contradictory but rather complementary.

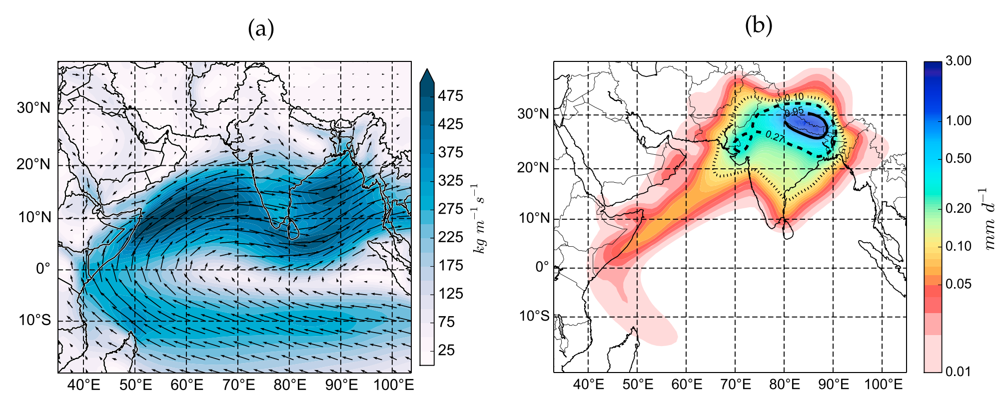

Figure 6. (a) Vertically integrated moisture flux from Era-Interim (1979–2010) averaged from June to September. (b) Moisture uptake for air parcels raining out over Nepal. The solid line encloses 25%, the stippled line 50%, and the dotted line 75%. Note that the color bar is logarithmic.

Table 1
Contribution to the Total Moisture Supply and, in Parentheses, the Positive Moisture Anomaly (in Percent) for Selected Countries on the Moisture Pathway for Extreme Precipitation Events

Country/region	Nepal	Cluster 1	Cluster 2	Cluster 3
Nepal	12	6 (0)	10 (5)	5 (3)
Pakistan	4	11 (14)	5 (6)	5 (6)
India	38	49 (52)	48 (56)	49 (57)
Over land	80	77 (75)	76 (76)	73 (74)
Bay of Bengal	5	3 (2)	4 (2)	5 (3)
Arabian Sea	15	20 (22)	20 (22)	22 (24)
Southern Hemisphere	3	4 (5)	4 (4)	4 (4)

6. Synoptic Conditions Characterizing Region-Specific Extreme Events

6.1. Composite Analysis

After introducing the mean state of the Indian summer monsoon, regarding atmospheric circulation and moisture sources for Nepal, we continue to discuss the distinctive features characterizing extreme precipitation events. We test whether Era-Interim can qualitatively reproduce the extreme precipitation events over the respective cluster areas (section 4). Figure 7 depicts Era-Interim total precipitation composites for the dates of extreme precipitation for each cluster. For the dates of extreme precipitation Era-Interim produces a significant amount of rainfall over the cluster regions. Central Nepal receives substantial precipitation in all cases, consistent with the general precipitation distribution in Nepal (Bohlinger & Sorteberg, 2017). We suggest that Era-Interim is capable of reproducing extreme precipitation events at the locations of the clusters. The result further indicates that mechanisms leading to extreme precipitation are governed by grid-scale features and the synoptic conditions which we focus on are represented well enough for further investigations.

We identify synoptic flow patterns for each cluster connected to the extremes. The flow in the vicinity of the clusters is directed toward the respective cluster at the day of the extreme event throughout most of the troposphere, illustrated for 500 hPa and 850 hPa (Figure 8). For cluster 1 the trough in midtroposphere is steep and points toward the Himalayas (Figure 8a). For clusters 2 and 3, the trough becomes more elongated and the flow turns gradually toward the cluster regions (Figures 8b and 8c). Similarly, in the lower troposphere low geopotential height stretches from Pakistan southeast along the Himalayas toward Bangladesh. The shape and extent of this low geopotential height region changes from cluster 1 to 3 to become more aligned with the Himalayas (Figures 8d–8f).

Across the middle and lower troposphere, a dipole structure consisting of a center of high and low anomaly supports the direction of the flow to the respective cluster region (Figure 8). For clusters 2 and 3 the flow needs to travel along the Himalayas and veer to the north farther east compared to cluster 1. This is reflected in the anomalies that support the respective flow patterns by their location, shape, and strength. In the middle

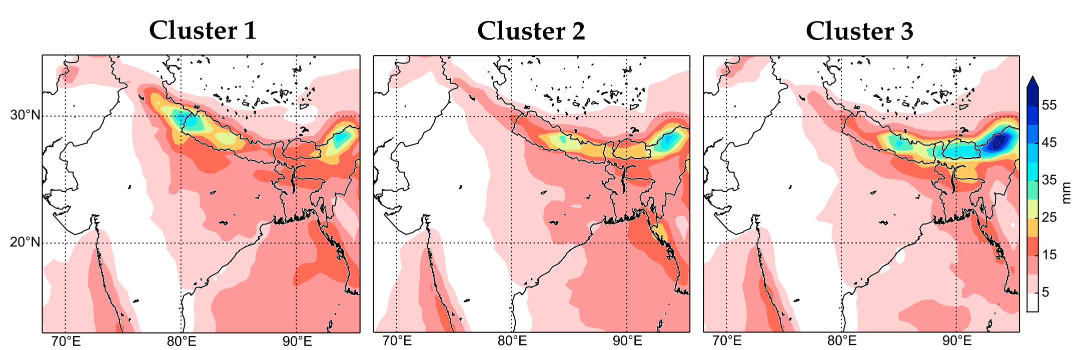

Figure 7. Composites of total precipitation from Era-Interim for all dates of extreme precipitation for cluster 1, cluster 2, and cluster 3. Daily amounts are displayed where the average is taken from 6 a.m. of the day before to 6 a.m. when the event is recorded. This adjustment was done to account for the time zone of Nepal.

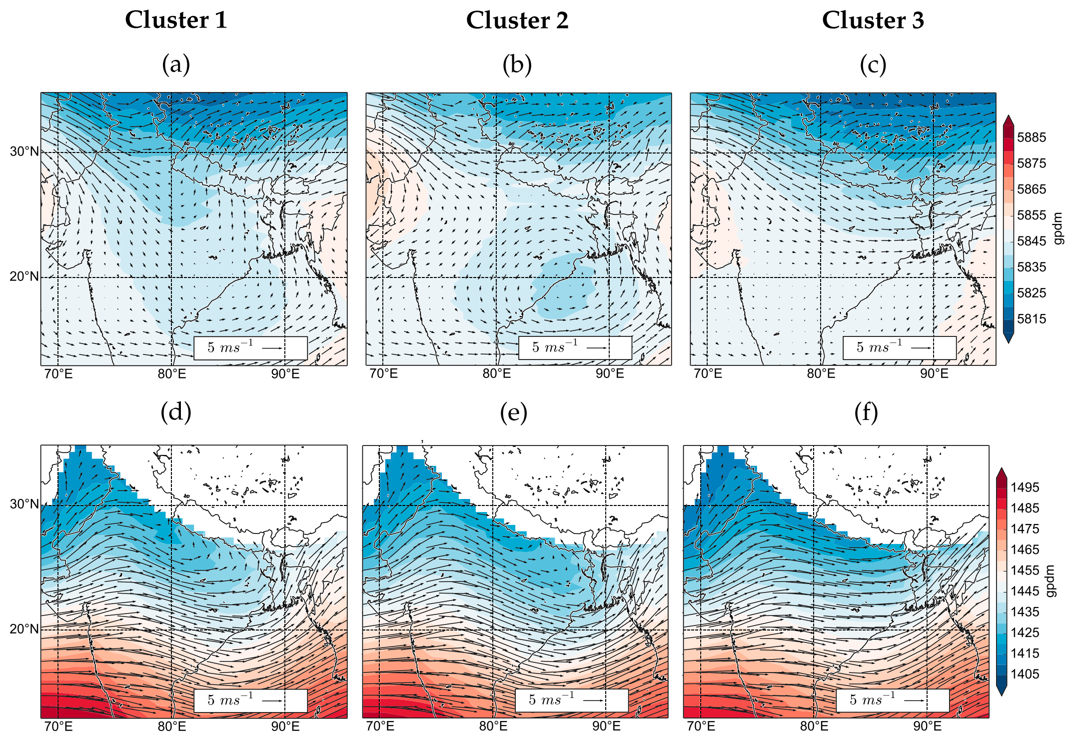

Figure 8. Era-Interim geopotential height at 500 hPa averaged over all extreme precipitation events for the period 1979–2010 from June to September for (a) cluster 1, (b) cluster 2, and (c) cluster 3. (d–f) The same but at 850 hPa. The arrows indicate the wind at the corresponding height.

and upper troposphere at (500 hPa and 300 hPa) pronounced anomaly patterns help to guide the flow toward the respective cluster region (Figures 9a–9g) which is much like the trough structure in Figures 8a–8c. The anomaly shows an increased north-south gradient with a negative anomaly trough at the location of cluster 1. Additionally, a positive anomaly region over northeast India forces the flow more northward, and enhanced winds are directed toward the Himalayas. For clusters 2 and 3 an elongated band of positive geopotential anomaly extends from Pakistan across India to Myanmar and Thailand. The positive anomaly is more pronounced for cluster 3 than for cluster 2 supporting the flow to be parallel to the mountains for a longer distance such that the flow does not turn north before east Nepal is reached. Our anomaly composites for central and east Nepal are consistent with results from Romatschke and Houze (2011) who found a negative geopotential height anomaly at 500 hPa across the Himalayas and south of the mountain chain, a positive anomaly prevailing during the occurrence of medium convective systems over the central Himalayan foothills. While their findings include all of Nepal, we resolve distinctive features characteristic for regions of Nepal revealing that the flow toward the Himalayas seems to be crucial for extreme precipitation events.

6.2. Variability Within the Cluster Composites

The composite analysis indicates that synoptic conditions guide the atmospheric flow to the Himalayas and consequently drain the available moisture due to orographic uplifting. Based on the 180 considered cases, various weather features can be associated with extreme precipitation events recorded at the stations. Prominent synoptic conditions are the following: a trough over the Himalayas (Figures 8 and 11), a low-pressure system from the Bay of Bengal (Figure 10), and sometimes, although less common, a low-pressure system from the Arabian Sea (Figure 10, right).

Monsoon LPS are known to mainly develop in the Bay of Bengal and travel to the north or northwest where some of them recurve to the east (Krishnamurthy & Ajayamohan, 2010; Sørland & Sorteberg, 2015b; Tyagi et al., 2012). We tracked all LPS (section 3.2) that entered a target region around Nepal and were existing during an extreme event (Figure 10). Most LPS relevant for extreme precipitation events in Nepal develop in the Bay of Bengal and move northwest where some recurve toward the northeast and east. Despite the difference in the number of extreme precipitation events for each cluster, the number of LPS that were present varied only little: 9 LPS for cluster 1 (18%), 11 LPS for cluster 2 (14%), and 11 LPS for cluster 3 (21%). LPS being

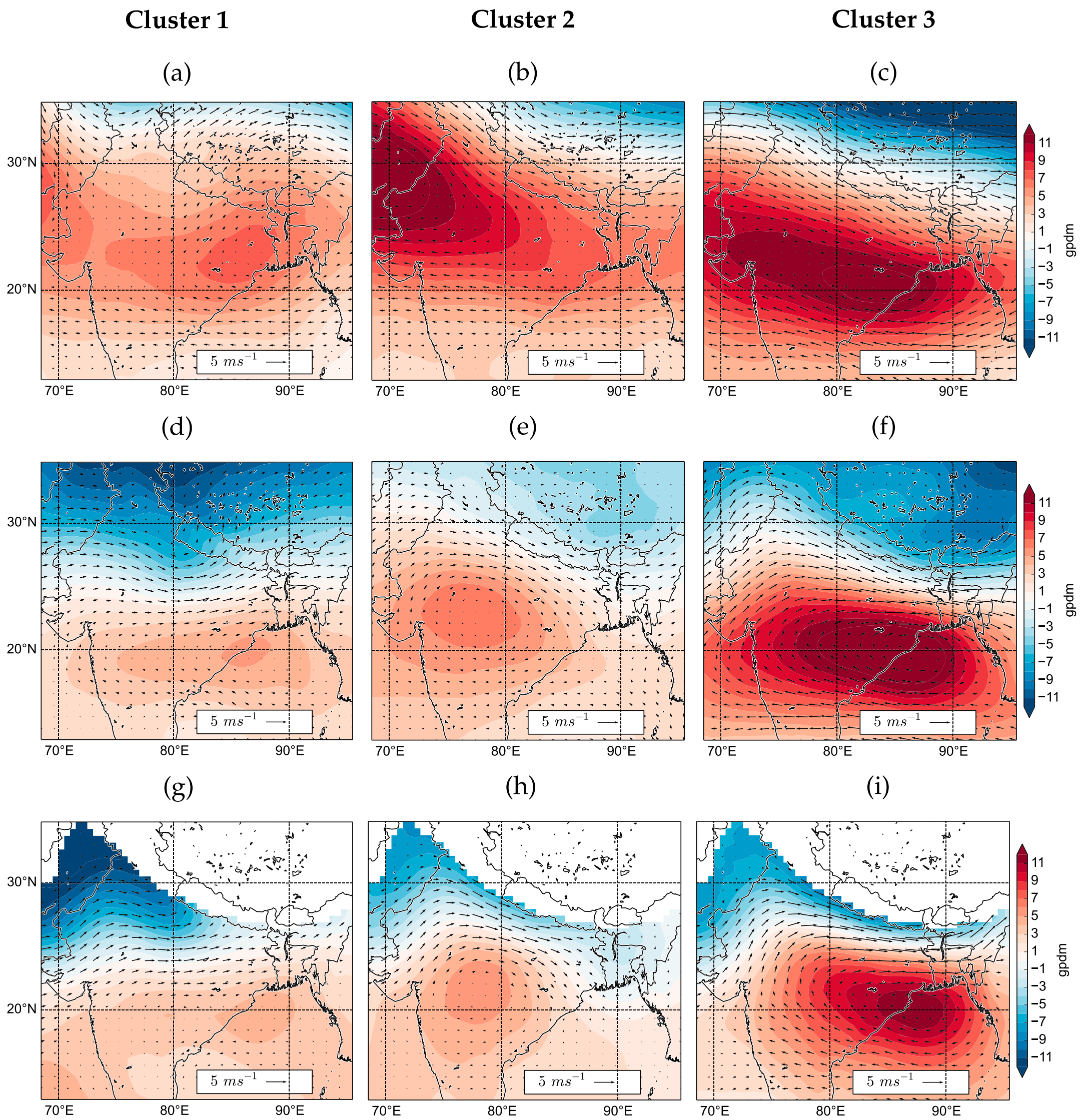

Figure 9. Geopotential height anomalies at 300 hPa from Era-Interim averaged for the period 1979–2010 from June to September for (a) cluster 1, (b) cluster 2, and (c) cluster 3. The same for (d–f) 500 hPa and (g–i) 850 hPa. The arrows indicate the wind anomalies at the corresponding height.

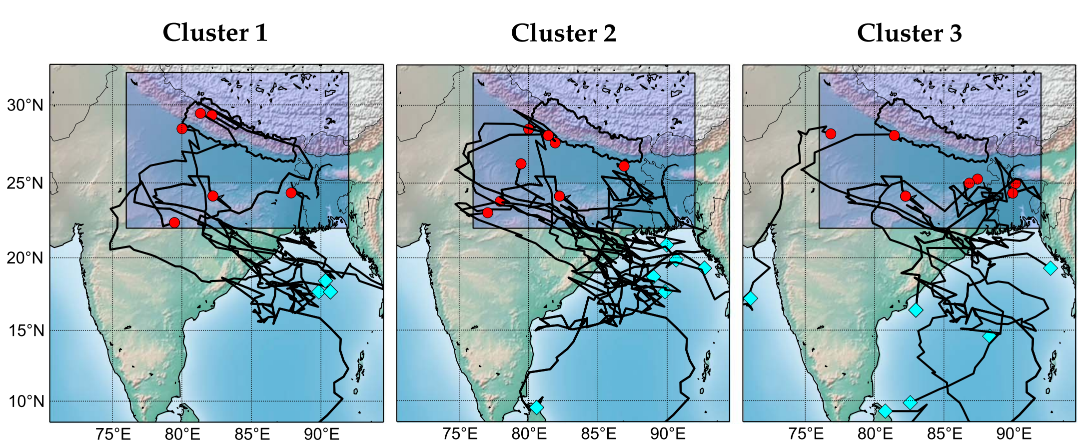

Figure 10. Trajectories of monsoon LPS that come close to Nepal during an extreme event. The blue boxes represent the target region for the LPS. Only LPS residing in this target region during an extreme event are tracked. The blue diamond represents the starting point and the red dot the end. Cluster 1: 9 LPS, Cluster 2: 11 LPS, Cluster 3: 11 LPS

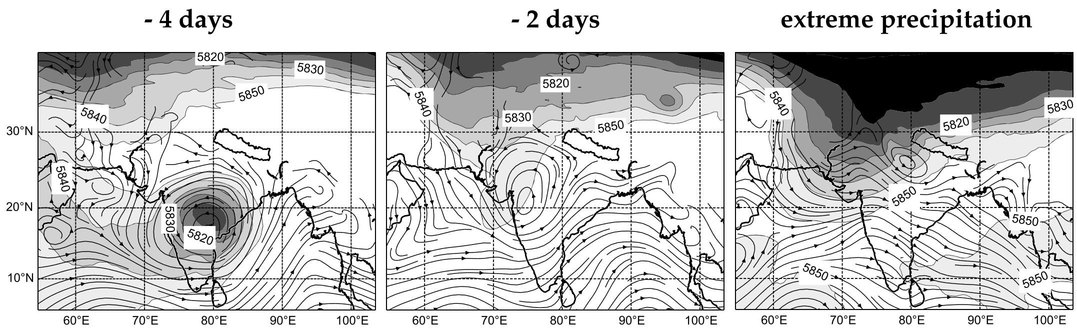

Figure 11. Streamlines illustrating the atmospheric flow field on 850 hPa prior to an extreme precipitation event in west Nepal on 25 September 2005. Contours represent the geopotential height at 500 hPa.

in the target region during extreme events in clusters 1 and 2 are characterized by a course farther west over India and end up close to west Nepal. For cluster 3, most are heading to the north, not undergoing the described recurving and end up close to the cluster region in east Nepal. We find that for our cases a trough structure with the accompanying wind field in the midtroposphere contributed to guide the LPS to the north which we will elaborate on in the following.

An example of those interactions is the low-pressure system that caused extreme precipitation in west Nepal on 25 September 2005 (Figure 11). Originating in the Bay of Bengal, a low-pressure system reached the Indian west coast 2 days prior to the extreme event and was redirected to Nepal guided by a midlevel trough. Two days prior to the event, the system had weakened, however, when the trough and the low-pressure system started to interact with the storm-shifted direction veering to the north and produced significant precipitation amounts, exceeding the 99.5 precentile at multiple rain gauges in western Nepal. We find that the interaction between troughs and monsoon LPS is closely connected to extreme precipitation events in Nepal.

6.3. Discussion of the Synoptic Conditions

The fact that midtropospheric troughs coincide with the extreme events in Nepal is consistent with other studies summarized in Tyagi et al. (2012). They found that these troughs considerably influence synoptic systems and rainfall during the Indian summer monsoon, for example, by triggering and intensifying LPS and subsequently increasing rainfall. Westerly troughs can also support guidance to LPS and can cause storms to recurve from their originally northwest course to the north or northeast (section 4.4 in Wang, 2005; Tyagi et al., 2012). Martius et al. (2013) described the effect of an upper level positive potential vorticity anomaly on the Pakistan flood of 2010, close to the area of cluster 1. Although the vorticity anomaly exerted quasi-geostrophic forcing on the affected region, its main effect was to orient the lower troposphere wind field toward the Himalayas causing orographic uplift.

In our study, for all three cluster regions the orientation of the wind field and the orographic uplift seem to play a major role. We identified the orographic uplift along the air parcels retrieved from the trajectory data set from Läderach and Sodemann (2016). Entering the region of clusters 1 and 2, air parcels rise on average over 2,000 m during their last two time steps (12 h) prior to their respective extreme event. For cluster 3 an uplift of similar magnitude takes place more gradually, happening over the last 5–10 time steps (30 h–60 h). This is consistent with the orientation of the flow which is directed more perpendicular to the mountain chain for clusters 1 and 2, whereas for extreme events in cluster 3, the flow in the lower and middle troposphere is oriented almost parallel to the Himalayas (Figure 8).

Besides features consistent with literature mentioned above, the meteorological context of the described extreme events differ considerably from those accompanying the floods in India and Pakistan (Kumar et al., 2014; Martius et al., 2013; Rasmussen & Houze, 2012). These studies consistently describe a blocking high over the Tibetian Plateau which together with monsoon LPS creates an increased pressure gradient generating an easterly jet along the Himalayas which transports moist air from the Bay of Bengal to the precipitating regions. In our case, this feature appears to be reversed. The gradient across the Himalayan mountain barrier is increased in our cases as well. However, we observe the atmospheric flow not being easterly but westerly before turning north and rising up the Himalayas. This result stresses the spatial variations inherent in extreme precipitation events along the Himalayas.

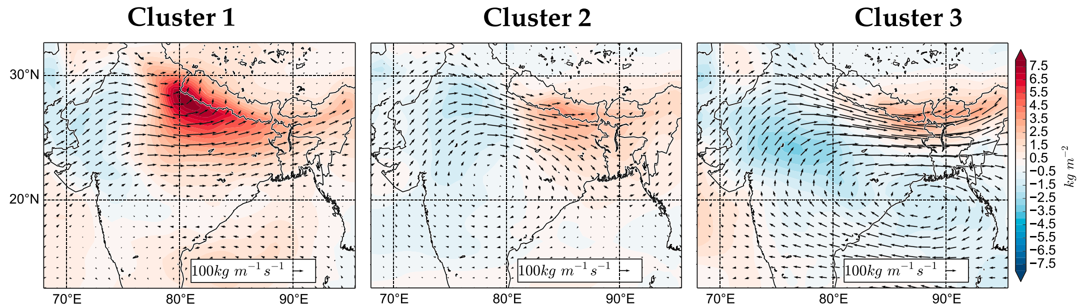

Figure 12. Vertically integrated moisture flux anomaly (arrows) composites for all extremes in the respective clusters. Total column moisture anomalies are displayed in contours.

Houze et al. (2007) and Medina et al. (2010) find evidence for continental air coming down from the Afghan Plateau, capping low-level moist air and consequently preventing premature convection. This is consistent with Sawyer (1947) who described this feature in a conceptual sketch. The composites in our study reveal a similar pattern where the flow in the high and middle troposphere emanates down from the Afghan Plateau when at the same time low-level air travels from the Arabian Sea over the Indus valley and veers to the east. The strength and the covered distance of the midlevel flow coincides with the location of the extreme events (Figures 8a–8c). Like in the conceptual sketch from Sawyer (1947), the continental air might contribute to prevent premature convection until the moisture is finally released at the location of the cluster. To assess this suggestion, a separate study would be needed to investigate the existence of a causal link (beyond the scope of this manuscript).

7. Moisture Flux and Moisture Sources

On days of extreme precipitation events, we find considerable positive total column moisture anomalies over the respective cluster regions (Figure 12). This is consistent with Barros and Lang (2003) who measured a peak in total column moisture and atmospheric instability just before an event. Vertically integrated moisture flux anomalies are directed to our cluster regions (Figure 12). For all cluster regions the moisture flux and its anomalies follow a similar path: coming from the Arabian Sea over northwest India to Bangladesh along the Himalayas until they turn to the north at the cluster regions. For the first cluster the moisture flux anomaly is directed north toward the Himalayas (Figure 12, left). For clusters 2 and 3 the moisture flux anomaly is directed parallel to the Himalayas until it gradually veers to the north toward the respective cluster regions (Figure 12, middle and right). The moisture flux is very similar to the anomalies (not shown).

The computed moisture sources for extreme precipitation events in the cluster regions mirror the pattern of moisture flux coming from the Arabian Sea and continuing along the Himalayas to the east. Moisture uptake occurs to a significant degree along the Indo-Gangetic Plain (Figure 13, and Figure 1 for orientation). For cluster 1, the core area of moisture uptake (solid black line indicating 25%) includes the area of extreme precipitation in Nepal together with a filament along the Indo-Gangetic Plain Figure 13a. For clusters 2 and 3 (Figures 13c and 13e) the 25th percentile is more concentrated around the cluster regions. For all clusters, roughly half of the moisture evaporated over the Indo-Gangetic Plain (stippled line). The rest of the accounted moisture stems from as far as the equator region at the east coast of Africa. Moisture over India is the largest contributor supplying half of moisture for extreme precipitation in Nepal, while Nepal adds 5–10% (Table 1). Although the magnitude of moisture uptake over Nepal is comparably large (blue colors in Figures 13a, 13c, and 13e), the area is limited and cannot match the moisture supply from India and Pakistan. In total, moisture uptake over land accounts for approximately 75% which is just slightly lower than the climatological value (Figure 6b and Table 1). The Bay of Bengal only plays a minor role, while the long tail and the reddish colors spreading over the Arabian Sea indicate some contribution from long-range transport. However, the fraction of moisture contribution from the Southern Hemisphere is marginal, which means that the budget-derived results assessing moisture sources and sinks for the Indian subcontinent (Cadet & Greco, 1987; Cadet & Reverdin, 1981; Wang, 2005) should be handled with caution when addressing precipitation and extreme precipitation in Nepal.

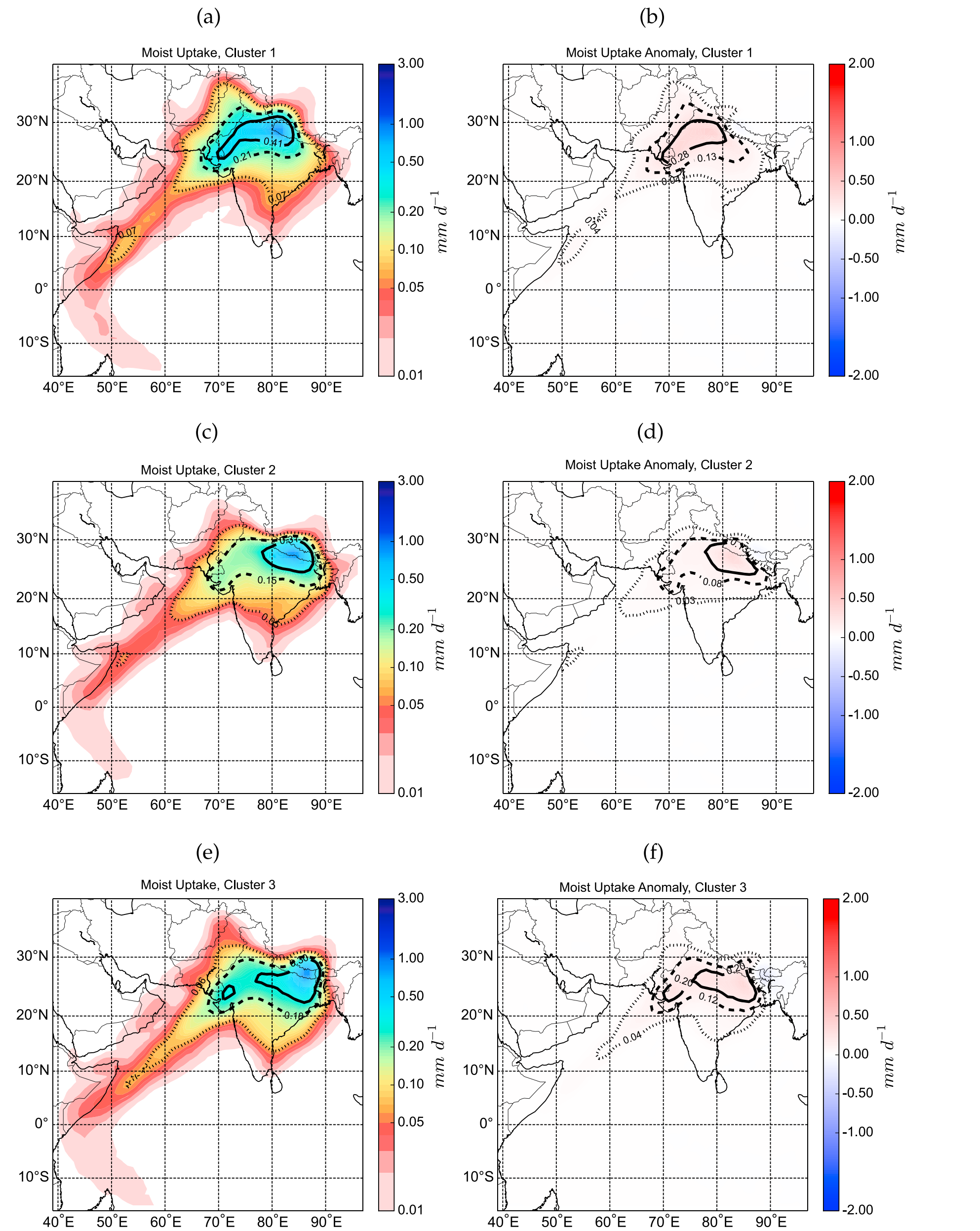

Figure 13. Composites of moisture uptake for extreme events in each cluster, (a) cluster 1, (c) cluster 2, and (e) cluster 3. (b, d, and f) The anomalies for these composites. The solid line encloses 25%, the stippled line 50%, and the dotted line 75% of the total uptake. For the anomalies, these lines enclose only positive contributions. Note that the color bars are logarithmic for Figures 13a, 13c, and 13e.

We computed moisture source anomalies to test whether there are different source regions or increased moisture uptake involved in extreme precipitation events over Nepal. The anomaly figures (Figures 13b, 13d, and 13f) underline the above discussed results that a considerable fraction of the additional uptake occurs over the cluster region and the Indo-Gangetic Plain. Interestingly, the region of cluster 1 is the only region where almost none of the additional moisture seems to stem from the cluster region itself (Figure 13c). In this region the atmospheric flow might interact with the terrain as soon as it comes close to the border of Nepal. Through the ascend it might be lifted above the defined threshold of 1.5 times the boundary layer height (section 3.3). In fact, when combining the contribution of the free troposphere and the boundary layer, a maximum over the cluster region appears (not shown). In complex terrain one should therefore be careful with interpreting the results of this method.

The largest positive moisture uptake anomaly is located over the Indo-Gangetic Plain. We find no region with a coherent negative uptake anomaly, whereas a positive anomaly can be observed across all of the major uptake regions. Compared to the monsoon mean, there appears to be no specific region with an increase in moisture contribution but rather a uniform increase of moisture uptake prior to the extreme events. The magnitude of the increase is related to the magnitude of the absolute contribution meaning that regions that generally contributed more, for example, the Indo-Gangetic Plain, also show the largest positive anomaly.

8. The Shape of the Moisture Source Patterns for Nepal

An important question that arises when exploring the moisture sources is the following: why is there moisture uptake over relatively dry regions like the Thar Desert in the Indus Plain (Figure 1)? Medina et al. (2010) pointed to the possibility of moisture uptake over land for heavy precipitation over Pakistan if the soil was moistened by a previous precipitation event. Martius et al. (2013) detected a large moisture contribution from land for the Pakistan flood in July 2010. They suggested the possibility of an intense coupling of precipitation and evapotranspiration but did not further address this issue. However, even if moisture is abundant, uptake will not be relevant for the extreme precipitation event if the air flow to the target region is not directed over the moist region.

The soil moisture depicts a considerable intraseasonal cycle where the Indian subcontinent is moistened as the monsoon matures. We illustrate this for extreme events in June and August as an example on the progression of the monsoon (Figures 14a and 14b). Northwest India, containing arid regions like the Thar Desert, experiences an increase of soil moisture which makes moisture uptake possible later in the monsoon season. A similar pattern is visible in the precipitation field (not shown). Romatschke et al. (2010) present results using the TRMM 3A25 product consistent with our findings. They conclude that for the Indus Plain the predominant convective precipitation features are deep convective and wide convective cores. Examples for intense precipitation events in the comparably dry uptake region along the Indus valley are described, for instance, in Houze et al. (2015, 2007) and Rasmussen et al. (2015). Due to a dry capping layer from the Afghan Plateau and Hindu Kush mountains, convection is usually inhibited, which is the reason for the prevalence of deep convective cores and wide convective cores in northwest India. Broad stratiform precipitation regions are not able to break through the capping layer unless they are exposed to forced lifting, for example, onto the Himalayan mountain barrier where they can be activated. In the context of three consecutive years of floods in Pakistan, Rasmussen et al. (2015) described intense, wide convective cores causing heavy precipitation over the arid region along the eastern border of Pakistan and the Indian states Gujarat and Rajasthan (Figure 1). Such intense convective events can moisten the otherwise dry region and might subsequently serve as moisture sources for extreme precipitation events in Nepal.

While the atmospheric flow changes throughout the season, extreme precipitation events depict considerable anomalies. To illustrate the seasonal changes, we choose extreme events in cluster 1 (Figures 14c and 14d). During extreme events in June the air crosses India almost zonally to veer to the north and northeast when reaching the Himalayas. In August there is a strong northward component from the Arabian sea, crossing Northwest India and veering to the east along the Himalayas. The flow anomalies might be influenced by break periods (section 9) resulting in the depicted pattern.

The progression of the soil moisture and the flow anomalies are reflected in the moisture sources (Figure 15) which exhibit a similar pattern. While the moisture sources for extreme events in June are close to the Bay of Bengal, moisture can be taken up over the dryer areas later in the monsoon season when soil moisture had already increased, for example, by the above described precipitation events. Not only does the uptake region change, but also the total amount of moisture that is taken up increases in August compared to June (Figure 15). For instance, the minimum and maximum daily amounts of all moisture taken up prior to an event which contributes to the respective extreme precipitation event ranges from 26 mm to 205 mm for June and from 34 mm to 383 mm for August. In August, the Indian summer monsoon is in a more mature state compared to June and has progressed far into the Indian subcontinent where precipitation events continuously increase the soil moisture content.

The last discussed factor that could be partly responsible for the shape of the moisture source pattern is irrigation. The Indo-Gangetic Plain is one of the strongest irrigated regions in the world (Siebert et al., 2005). Era-Interim indirectly accounts for irrigation by using surface observations of humidity and temperature to subsequently correct soil moisture (Douville et al., 2000; Wei et al., 2013). Wei et al. (2013) found that taking

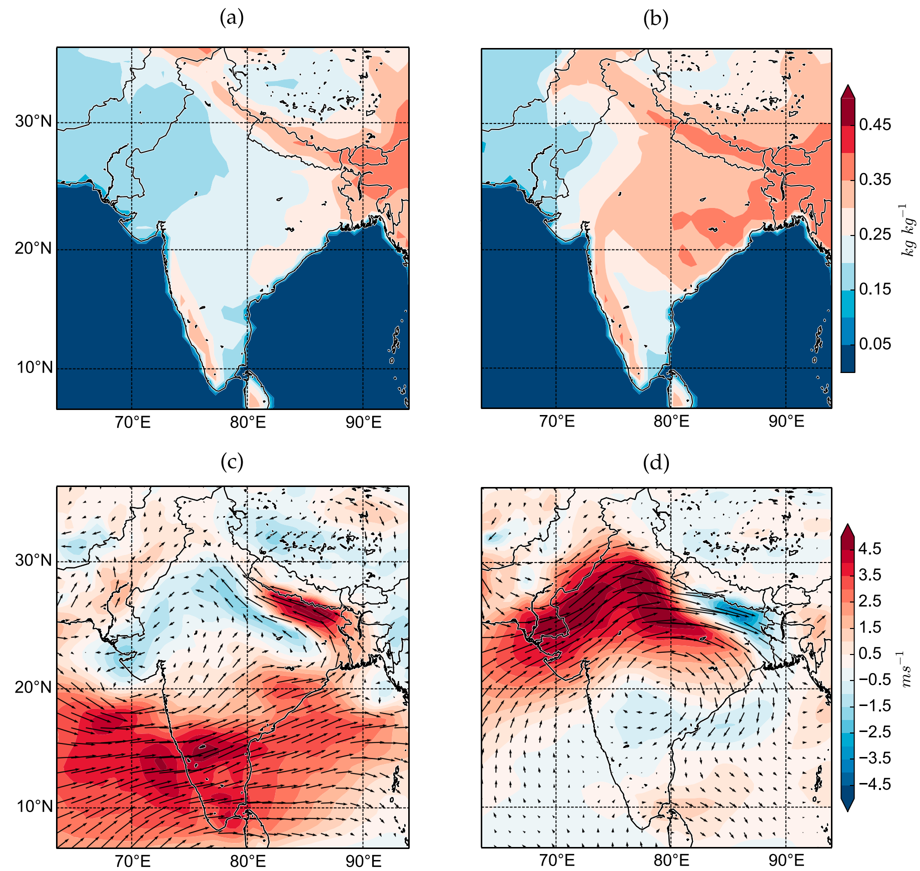

Figure 14. Monthly mean (1979–2010) Era-Interim soil moisture for (a) June and (b) August, and wind anomalies on 850 hPa for extreme events occurring in (c) June and (d) August.

irrigation into account significantly changes evaporation over the Indo-Gangtic plain up to 200% or 500 mm annually. They further state that up to 25% of the annual precipitation in this region could stem from the increased evaporation. These are significant contributions to the moisture uptake, and since Era-Interim supplies the boundary conditions for the used trajectories, the increased evaporation likely contributes to the increased uptake in our results and hence the shape of the moisture source pattern.

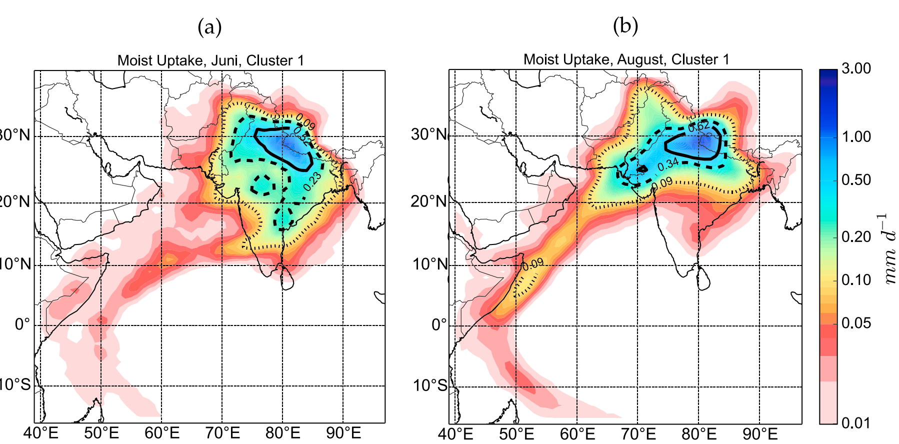

Figure 15. Moisture uptake for all extreme events at cluster 1 (a) in June and (b) in August. The solid line encloses 25%, the stippled line 50%, and the dotted line 75%. Note that the color bar is logarithmic.

Table 2
Contribution to the Total Moisture Supply for Rajasthan (in Percent) for Each Country That Exceeds a Contribution of 5%

Rajasthan	1–10 June	21–31 June
Pakistan	9	13
India	28	37
Over land	49	62
Arabian Sea	50	37
Southern Hemisphere	8	7

Note. To illustrate the temporal change, two periods are contrasted: 1–10 June and 21–30 June. Values for the chosen periods are averaged from 1979 to 2010.

We quantify the moisture sources for the dryer regions to extend our chain of argument regarding the above mentioned preconditioning precipitation events. We choose an area in the state Rajasthan in northwest India (Figure 1) as an example for an arid region which cannot offer much moisture in general. Nonetheless, we see uptake of moisture in this region for precipitation and extreme precipitation events in Nepal, also described by Martius et al. (2013) for the Pakistan flood 2010. Figure 14 indicates that in the beginning of June only little moisture precipitates out over this region. From this moisture the largest contributors are the Arabian Sea with 50% (Table 2) and southeast Pakistan together with the state Gujarat close to the Indus delta. Close to the delta, there are also lakes that could serve as moisture sources during the intense insolation in the Indian summer monsoon. The Southern Hemisphere contributes only 8%. This is, however, double the fraction compared to regions in Nepal. The increased contribution from moisture sources in the Southern Hemisphere is consistent with the argument of residence time. Following the moisture path, Rajasthan is roughly 1,000 km closer to the source regions in the Southern Hemisphere than much of Nepal (Figure 1). Hence, moisture taken up over the Southern Hemisphere needs to travel at least a day less assuming an average speed of 10 m s^{-1}, which also increases the probability that it does not rain out along the way.

By the end of June more moisture has been transported over land and precipitated over the arid regions such that uptake can occur. The land fraction increases due to the increased moisture availability, and India now contributes as much as the Arabian Sea with 37%. The occasional occurrence of precipitation in these dry regions is also present in Era-Interim (not shown). Era-Interim supplies the boundary data for the Lagrangian trajectories and makes our result in the presented framework physically consistent. Our result is also consistent with multiple studies that illustrated the occurrence of precipitation and intense rainstorms in this region (Houze et al., 2007, 2015; Rasmussen et al., 2015; Romatschke & Houze, 2011; Romatschke et al., 2010). A large fraction of moisture contributing to the Pakistan flood in 2010 came from the Arabian Sea (Houze et al., 2011; Martius et al., 2013).

9. Impact of Break Periods

A common feature often related to abnormal rainfall over the Himalayas and India are monsoon break periods which are defined by less rainfall over most of central India but more in the north and south of the country (Tyagi et al., 2012). Break periods have also been tied to heavy precipitation along the Himalayas (Nandargi & Dhar, 2011). A typical feature of monsoon break periods is a flow splitting west of India where the main branch curves around the southern edge of the subcontinent veering again to the north in the Bay of Bengal (Joseph & Sijikumar, 2004). A northern branch moves from the Arabian Sea to the northwest along the Himalayas. Our moisture source regions match the northern branch that prevails during monsoon break periods.

We test whether the dates of extreme precipitation in our study coincide with break periods based on the four studies compared in Rajeevan et al. (2010). The compared break periods are only listed for the months July and August and do not always overlap. Therefore, we count a date when it coincides with at least one of the defined periods. A noticeable fraction of the extreme events in July and August (cluster 1, 26%; cluster 2, 25%; and cluster 3, 43%) occurs during break periods. If we ease the constraint and allow a deviation of ± 1 day, bearing in mind the temporal differences that come along with the different definitions, this fraction increases drastically (cluster 1, 44%; cluster 2, 35%; and cluster 3, 57%). In total, we count 7 hits and 12 close hits for cluster 1, 13 hits and 18 close hits for cluster 2, and 15 hits and 20 close hits for cluster 3. Rajeevan et al. (2010) found that with their definition there are on average 7 days (11%) during July and August defined as break period. However, counting all days in July and August which are considered break periods in at least one study compared in Rajeevan et al. (2010), we find that on average 15 days (24%) is defined as a break period in July and August between 1951 and 1989. In Rajeevan et al. (2010), after 1989, there is only one study we can use for the identification of break periods which consequently leads to a lower hit rate. This means that the meaning of the break periods for the extreme events is likely underestimated. Hence, break periods during July and August appear to be related to extreme precipitation in Nepal and may influence the displayed pattern of moisture sources (Figure 13) and vertical integrated moisture transport (Figure 12).

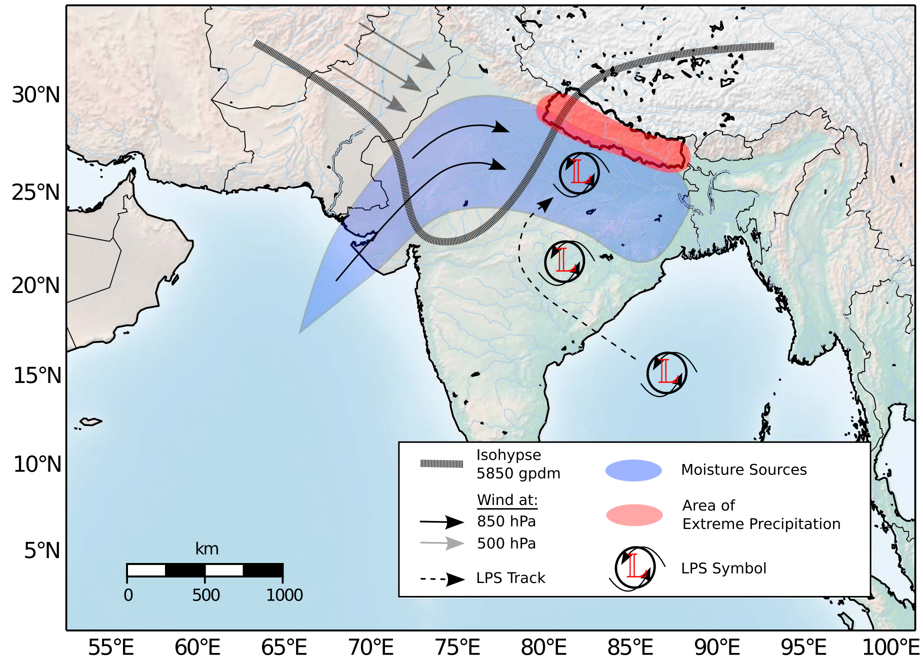

Figure 16. Conceptual sketch of processes leading to extreme precipitation in Nepal.

10. Conclusion

We systematically investigated and discussed synoptic conditions and moisture sources actuating extreme precipitation in Nepal for the time period from 1979 to 2010. The involved key processes are illustrated in Figure 16 which forms the basis for the following conclusion. Taking into account the high spatial variability in rainfall in Nepal through clustering, we revealed an interplay between different synoptic scale features that act to direct the atmospheric flow against the Nepalese Himalayas at the location of the extreme event. Although there are likely more processes involved, we focused on LPS and midlevel troughs. The midlevel trough could force a low-pressure system to change direction and ultimately lead it to Nepal where extreme precipitation occurred. This was illustrated for 25 September 2005 and is also evident in the composite analysis of the geopotential height and atmospheric flow together with the paths of the LPS. On average, 14%–21% of the extreme events were accompanied by LPS. The result from this long-term, composite approach is consistent with existing studies that have described the influence of troughs on the path of LPS investigating single events. In a composite analysis we found further a low-level flow from the Arabian Sea and midlevel flow from the Afghan Plateau. A resulting capping and retarded triggering of convection was described by Sawyer (1947), Houze et al. (2007), and Medina et al. (2010). We found indications that this process might be important for the location of extreme precipitation along the Nepalese Himalayas as well. Moisture uptake was increased prior to the extreme events explaining the origin of the emerging positive anomalies in moisture transport and total water vapor. We quantified major moisture sources and detected the main moisture uptake over land (approximately 75%) where India, Pakistan, and Nepal were major contributors. The most prominent uptake region was the Indo-Gangetic Plain where almost half of the precipitating moisture was taken up. The location of the moisture sources could be related to irrigation processes which are indirectly taken into account in Era-Interim. Another reason for the increased moisture uptake is the progression of the monsoon preconditioning the soil moisture for increased moisture uptake during anomalies in the low-level atmospheric flow. These anomalies were noticeably influenced by break period conditions in July and August. Between 35% and 57% of the events in July and August occurred close to or during a break period where this fraction is likely underestimated. Half of the moisture taken up in our example region in Rajasthan, representing dryer regions along the main uptake path, stemmed from the Arabian Sea in the beginning of June. Once the monsoon had matured, by the end of June, more moisture came from land (62%). Further numerical studies might help to disentangle the involved processes and shed more light on the role of moisture sources and their implications for extreme precipitation in Nepal.

Appendix A: Method Sensitivity

A challenge when dealing with observations is the presence of missing values. In terms of clustering there are two basic approaches: fill in missing values (imputation) or ignore them (marginalization). Since all stations used for the study have missing values in different time intervals, there would be a substantial loss of information when applying marginalization. Although in our case there are only 4% missing data, marginalization would result in a reduction of the data set by approximately 43%. With the aim to minimize the loss of information, we applied the imputation method. We acknowledge that clustering with missing values using no imputation is possible which is described, for instance, in Wagstaff (2004). However, from the findings of Wagstaff (2004) substituting with reasonable values, for example, using the mean, should be no drawback when only few data are missing. Introducing artificial values into a data set could distort the clustering results, which is why we performed a brief sensitivity tests on this issue. We tested different values for imputation as mean, median, and an arbitrary value. However, changing the substituted values resulted in negligible changes in cluster membership at the rims of the clusters.

Another factor that can influence the outcome of clustering is the chosen distance metric. We find that the clusters are little sensitive to changes in distance measures, meaning that only stations at the cluster rims might switch cluster memberships. Additionally, the sensitivity to changing the amount of clustered stations is very low; for example, clustering only the stations that have consistent records for all 40 years results in a very similar grouping of stations. Different distance measures like cosine or the city block metric were tested with similar outcomes.

Acknowledgments
This work has been funded by the University of Bergen, Norway. The authors thank the Department of Hydrology and Meteorology (DHM) in Nepal for sharing their rain gauge data set. ERA-Interim reanalyses were provided through the ECMWF data server. We would also like to thank Kevin Hodges, University of Reading, UK, for help with tracking the low-pressure systems.

References

Baidya, S., Shrestha, M., & Sheikh, M. (2008). Trends in daily climatic extremes of temperature and precipitation in Nepal. *Journal of Hydrology and Meteorology*, *5*(1), 38–51.

Barros, A., Joshi, M., Putkonen, J., & Burbank, D. (2000). A study of the 1999 monsoon rainfall in a mountainous region in central Nepal using TRMM products and rain gauge observations. *Geophysical Research Letters*, *27*(22), 3683–3686.

Barros, A. P., & Lang, T. J. (2003). Monitoring the monsoon in the Himalayas: Observations in central Nepal, June 2001. *Monthly Weather Review*, *131*(7), 1408–1427.

Bohlinger, P., & Sorteberg, A. (2017). A comprehensive view on trends in extreme precipitation in Nepal and their spatial distribution. *International Journal of Climatology*. https://doi.org/10.1002/joc.5299

Bookhagen, B., & Burbank, D. W. (2006). Topography, relief, and TRMM-derived rainfall variations along the Himalaya. *Geophysical Research Letters*, *33*, L08405. https://doi.org/10.1029/2006GL026037

Bookhagen, B., & Burbank, D. W. (2010). Toward a complete Himalayan hydrological budget: Spatiotemporal distribution of snowmelt and rainfall and their impact on river discharge. *Journal of Geophysical Research*, *115*, F03019. https://doi.org/10.1029/2009JF001426

Cadet, D. L., & Greco, S. (1987). Water vapor transport over the Indian Ocean during the 1979 summer monsoon. Part II: Water vapor budgets. *Monthly Weather Review*, *115*(10), 2358–2366. https://doi.org/10.1175/1520-0493(1987)115<2358:WVTOTI>2.0.CO;2

Cadet, D., & Reverdin, G. (1981). Water vapour transport over the Indian Ocean during summer 1975. *Tellus*, *33*(5), 476–487.

Caesar, J., Alexander, L., Trewin, B., Tse-ring, K., Sorany, L., Vuniyayawa, V., … Sirabaha, S. (2011). Changes in temperature and precipitation extremes over the Indo-Pacific region from 1971 to 2005. *International Journal of Climatology*, *31*(6), 791–801. https://doi.org/10.1002/joc.2118

Chalise, S., & Khanal, N. (2002). Recent extreme weather events in the Nepal Himalayas, *The extremes of the extremes: Extraordinary floods* (Vol. 271, pp. 141–146). Iceland: IHAS Publ. no. 271.

Dee, D., Uppala, S., Simmons, A., Berrisford, P., Poli, P., Kobayashi, S., … Vitart, F. (2011). The ERA-Interim reanalysis: Configuration and performance of the data assimilation system. *Quarterly Journal of the Royal Meteorological Society*, *137*(656), 553–597.

Douville, H., Viterbo, P., Mahfouf, J.-F., & Beljaars, A. C. (2000). Evaluation of the optimum interpolation and nudging techniques for soil moisture analysis using FIFE data. *Monthly Weather Review*, *128*(6), 1733–1756. https://doi.org/10.1175/1520-0493(2000)128<1733:EOTOIA>2.0.CO;2

Ghosh, S., Pant, M., & Dewan, B. (1978). Influence of the Arabian Sea on the Indian summer monsoon. *Tellus*, *30*(2), 117–125.

Hannah, D. M., Smith, B. P., Gurnell, A. M., & McGregor, G. R. (2000). An approach to hydrograph classification. *Hydrological Processes*, *14*(2), 317–338.

Hodges, K. (1995). Feature tracking on the unit sphere. *Monthly Weather Review*, *123*(12), 3458–3465.

Hodges, K. (1999). Adaptive constraints for feature tracking. *Monthly Weather Review*, *127*(6), 1362–1373.

Hodges, K. I. (1994). A general method for tracking analysis and its application to meteorological data. *Monthly Weather Review*, *122*(11), 2573–2586.

Houze, Jr., Rasmussen, K., Medina, S., Brodzik, S., & Romatschke, U. (2011). Anomalous atmospheric events leading to the summer 2010 floods in Pakistan. *Bulletin of the American Meteorological Society*, *92*(3), 291–298. https://doi.org/0.1175/2010BAMS3173.1

Houze, Jr., Rasmussen, K. L., Zuluaga, M. D., & Brodzik, S. R. (2015). The variable nature of convection in the tropics and subtropics: A legacy of 16 years of the Tropical Rainfall Measuring Mission satellite. *Reviews of Geophysics*, *53*, 994–1021. https://doi.org/10.1002/2015RG000.488

Houze, Jr., Wilton, D. C., & Smull, B. F. (2007). Monsoon convection in the Himalayan region as seen by the TRMM Precipitation Radar. *Quarterly Journal of the Royal Meteorological Society*, *133*(627), 1389–1411. https://doi.org/10.1002/qj.106

Ichiyanagi, K., Yamanaka, M. D., Muraji, Y., & Vaidya, B. K. (2007). Precipitation in Nepal between 1987 and 1996. *International Journal of Climatology*, *27*(13), 1753–1762. https://doi.org/10.1002/joc.1492

Joseph, P., & Sijikumar, S. (2004). Intraseasonal variability of the low-level jet stream of the Asian summer monsoon. *Journal of Climate*, *17*(7), 1449–1458. https://doi.org/10.1175/1520-0442(2004)017<1449:IVOTLJ>2.0.CO;2

Kansakar, S. R., Hannah, D. M., Gerrard, J., & Rees, G. (2004). Spatial pattern in the precipitation regime of Nepal. *International Journal of Climatology*, *24*(13), 1645–1659.

Krishnamurthy, V., & Ajayamohan, R. (2010). Composite structure of monsoon low pressure systems and its relation to Indian rainfall. *Journal of Climate*, *23*(16), 4285–4305. https://doi.org/10.1175/2010JCLI2953.1

Kumar, A., R. A. Houze, Jr, Rasmussen, K. L., & Peters-Lidard, C. (2014). Simulation of a flash flooding storm at the steep edge of the Himalayas. *Journal of Hydrometeorology*, *15*(1), 212–228. https://doi.org/10.1175/JHM-D-12-0155.1

Läderach, A. (2016). Characteristic scales of atmospheric moisture transport (PhD thesis), ETH Zurich.

Läderach, A., & Sodemann, H. (2016). A revised picture of the atmospheric moisture residence time. *Geophysical Research Letters*, *43*, 924–933. https://doi.org/10.1002/2015GL067449

Lang, T. J., & Barros, A. P. (2002). An investigation of the onsets of the 1999 and 2000 monsoons in central Nepal. *Monthly Weather Review*, *130*(5), 1299–1316. https://doi.org/10.1175/1520-0493(2002)130<1299:AIOTOO>2.0.CO;2

Martius, O., Sodemann, H., Joos, H., Pfahl, S., Winschall, A., Croci-Maspoli, M., … Wernli, H. (2013). The role of upper-level dynamics and surface processes for the Pakistan flood of July 2010. *Quarterly Journal of the Royal Meteorological Society*, *139*(676), 1780–1797. https://doi.org/10.1002/qj.2082

Medina, S., Houze, R. A., Kumar, A., & Niyogi, D. (2010). Summer monsoon convection in the Himalayan region: Terrain and land cover effects. *Quarterly Journal of the Royal Meteorological Society*, *136*(648), 593–616. https://doi.org/10.1002/qj.601

Nandargi, S., & Dhar, O. (2011). Extreme rainfall events over the Himalayas between 1871 and 2007. *Hydrological Sciences Journal*, *56*(6), 930–945. https://doi.org/10.1080/02626667.2011.595373

Nayava, J. L. (1980). Rainfall in Nepal. *Himalayan Review*, *12*, 1–18.

Rajeevan, M., Gadgil, S., & Bhate, J. (2010). Active and break spells of the Indian summer monsoon. *Journal of Earth System Science*, *119*(3), 229–247.

Rasmussen, K., Hill, A., Toma, V., Zuluaga, M., Webster, P., & Houze, R. (2015). Multiscale analysis of three consecutive years of anomalous flooding in Pakistan. *Quarterly Journal of the Royal Meteorological Society*, *141*(689), 1259–1276. https://doi.org/10.1002/qj.2433

Rasmussen, K. L., & Houze, Jr. (2012). A flash-flooding storm at the steep edge of high terrain: Disaster in the Himalayas. *Bulletin of the American Meteorological Society*, *93*(11), 1713–1724. https://doi.org/10.1175/BAMS-D-11-00236.1

Romatschke, U., & Houze, Jr. (2011). Characteristics of precipitating convective systems in the South Asian monsoon. *Journal of Hydrometeorology*, *12*(1), 3–26.

Romatschke, U., Medina, S., & Houze, Jr. (2010). Regional, seasonal, and diurnal variations of extreme convection in the South Asian region. *Journal of Climate*, *23*(2), 419–439.

Rousseeuw, P. J. (1987). Silhouettes: A graphical aid to the interpretation and validation of cluster analysis. *Journal of Computational and Applied Mathematics*, *20*, 53–65.

Sawyer, J. (1947). The structure of the intertropical front over NW India during the SW monsoon. *Quarterly Journal of the Royal Meteorological Society*, *73*(317–318), 346–369. https://doi.org/10.1002/qj.49707331709

Shrestha, A. B., Bajracharya, S. R., Sharma, A. R., Duo, C., & Kulkarni, A. (2016). Observed trends and changes in daily temperature and precipitation extremes over the Koshi river basin 1975–2010. *International Journal of Climatology*, *37*, 1066–1083. https://doi.org/10.1002/joc.4761

Siebert, S., Döll, P., Hoogeveen, J., Faures, J.-M., Frenken, K., & Feick, S. (2005). Development and validation of the global map of irrigation areas. *Hydrology and Earth System Sciences Discussions*, *2*(4), 1299–1327.

Sodemann, H., Schwierz, C., & Wernli, H. (2008). Interannual variability of Greenland winter precipitation sources: Lagrangian moisture diagnostic and North Atlantic Oscillation influence. *Journal of Geophysical Research*, *113*, D03107. https://doi.org/10.1029/2007JD008503

Sørland, S. L., & Sorteberg, A. (2015a). The dynamic and thermodynamic structure of monsoon low-pressure systems during extreme rainfall events. *Tellus A: Dynamic Meteorology and Oceanography*, *67*, 27039. https://doi.org/10: 3402/tellusa.v67.27039

Sørland, S. L., & Sorteberg, A. (2015b). Low-pressure systems and extreme precipitation in central India: Sensitivity to temperature changes. *Climate Dynamics*, *47*(1–2), 465–480. https://doi.org/10.1007/s00382-015-2850-4

Stohl, A., Forster, C., Frank, A., Seibert, P., & Wotawa, G. (2005). Technical note: The Lagrangian particle dispersion model FLEXPART version 6.2. *Atmospheric Chemistry and Physics*, *5*(9), 2461–2474. https://doi.org/10.5194/acp-5-2461-2005

Tibshirani, R., Walther, G., & Hastie, T. (2001). Estimating the number of clusters in a data set via the gap statistic. *Journal of the Royal Statistical Society: Series B (Statistical Methodology)*, *63*(2), 411–423.

Trenberth, K. E., Dai, A., Rasmussen, R. M., & Parsons, D. B. (2003). The changing character of precipitation. *Bulletin of the American Meteorological Society*, *84*(9), 1205–1217. https://doi.org/10.1175/BAMS-84-9-1205

Tyagi, A., Asnani, P., De, U., Hatwar, H., & Mazumdar, A. (2012). *The monsoon monograph* (Vol. 1 and 2): Indian Meteorological Department.

Wagstaff, K. (2004). *Clustering with missing values: No imputation required*. New Delhi: India Meteorological Department Mausam Bhavan.

Wang, E. B. (2005). *The Asian monsooon*. New York: Springer/Praxis Publishing Co.

Wei, J., Dirmeyer, P. A., Wisser, D., Bosilovich, M. G., & Mocko, D. M. (2013). Where does the irrigation water go? An estimate of the contribution of irrigation to precipitation using MERRA. *Journal of Hydrometeorology*, *14*(1), 275–289. https://doi.org/10.1175/JHM-D-12-079.1

Winschall, A., Pfahl, S., Sodemann, H., & Wernli, H. (2014). Comparison of Eulerian and Lagrangian moisture source diagnostics—The flood event in eastern Europe in May 2010. *Atmospheric Chemistry and Physics*, *14*(13), 6605–6619. https://doi.org/doi:10.5194/acp-14-6605-2014